Evaluation of North Atlantic Property Field Simulations at ⅙°

YI CHAO

Jet Propulsion Laboratory, California Institute of Technology, Pasadena, California

M. SUSAN LOZIER

Earth and Ocean Sciences, Duke University, Durham, North Carolina

ABSTRACT

One way to measure the skill of an ocean general circulation model is to evaluate its ability to simulate observed property distributions. Pressure, temperature, and salinity distributions generated by a ⅙° Atlantic Ocean general circulation model are compared with climatological fields on three potential density surfaces, representative of the upper, middepth, and deep ocean waters. The upper ocean property fields are relatively well simulated, a testimony to the model's ability to generally reproduce the wind-driven circulation in the North Atlantic. However, in the middepth and deep ocean, where wind forcing is negligible and buoyant flows associated with deep-water formation play a major role in establishing property distributions, the fields are poorly represented in the ⅙° Atlantic Ocean model. The comparison between the observed and modeled fields indicates several model deficiencies in the representation of intermediate and deep waters and their pathways. Possible model improvements to reduce the mismatch between model and data are proposed.

1. Introduction

North Atlantic Ocean general circulation models have substantially improved during the last decade. Extensive model sensitivity experiments have been conducted to improve surface boundary conditions, to explore the role of horizontal resolution, and to improve the choice of model parameters. Many of these studies have been conducted as part of the World Ocean Circulation Experiment's U.S.–German Community Modeling Effort (Bryan and Holland 1989) and the European Union Marine Science and Technology's Dynamics of North Atlantic Models (DYNAMO) project (DYNAMO Group 1997; Willebrand et al. 2001). The recent advent of parallel computing technology has allowed for ocean modeling at spatial resolutions of ¼° (Semtner and Chervin 1988), ⅙° (Smith et al. 1992; Beckmann et al. 1994; Chao et al. 1996), $\frac{1}{10}$° (Smith et al. 2000), and $\frac{1}{12}$° (Paiva et al. 1999). Because of the high computational costs required, these high-resolution models have been integrated for only a few decades. While this integration length is sufficient for the upper ocean to reach dynamical equilibrium, it is clearly not sufficient for thermodynamic equilibrium, particularly in the deep ocean. Thus, efforts toward the validation of these high-reso-

lution model simulations have primarily focused on features of the velocity field, such as the distribution of mean and eddy kinetic energy, the Gulf Stream separation from the western boundary, and mass and heat transports. However, the ultimate goal of ocean general circulation modeling (Semtner 1995; McWilliams 1995) is to reproduce not only features of the velocity field, but property field distributions as well. Understanding how properties are distributed within a basin, and eventually over the global ocean, is key to our understanding of climatic processes in the ocean. Because the distribution of a property depends largely on the integrative effects of the flow field, a model's ability to simulate observed property distributions would affirm its balance between advection and diffusion, its prescription of boundary conditions, and its partitioning between mean and eddy components.

This study evaluates the property field distributions simulated by a ⅙° Atlantic Ocean general circulation model (Chao et al. 1996; Carton and Chao 1999; Nakamura and Chao 2001) that has been integrated for 34 years. We have chosen to evaluate an eddy-resolving model's ability to simulate the observed property fields because we believe that eddies play an important role in the distribution of properties. This is true not only in the surface waters, but also at depth where eddy-driven flow can sometimes dominate the flow field (Lozier 1997). Thus, we anticipate that as computing power grows, eddy-resolving models run to thermodynamic

Corresponding author address: Dr. Yi Chao, Jet Propulsion Laboratory, California Institute of Technology, 4800 Oak Grove Dr., MS 300-323, Pasadena, CA 91109.
E-mail: yi.chao@jpl.nasa.gov

equilibrium will be used for climate studies. Although the current computing power precludes the integration of this model to a full thermodynamical equilibrium, it is instructive to compare the modeled property fields with the climatological fields after a dynamical equilibrium has been reached (on the order of a few decades). Though we recognize that the model fields in full thermodynamical equilibrium may differ from the model fields after our 34-yr integration, we believe coarse differences between the modeled and observed fields in the early stages of a thermodynamic equilibrium can signal model deficiencies in initial conditions and boundary conditions. It is important to recognize and address these model deficiencies because the use of eddy-resolving ocean circulation models for climate studies hinges on their ability to reproduce the known water mass distribution. To justify our approach, we have compared the deep property fields from a coarse-resolution model (Gent et al. 1998) that has reached thermodynamic equilibrium to those property fields at an intermediate integration stage (M. Hecht 2001, personal communication). From this comparison it was apparent that model discrepancies could be detected before a full thermodynamic equilibrium was reached.

With this model and data comparison, we address the following questions:

- Are water masses being formed and spread in the model ocean?
- To what extent do the model's water masses differ from the observed water masses in terms of gross property (temperature and salinity) strength, horizontal spread, and depth of penetration?
- What is the relative location and strength of the modeled water masses?

With the overall goal of improving the model's thermohaline circulation, this preliminary study represents a realistic first step toward establishing thermodynamic similarities and differences between eddy-resolving ocean model simulations and observations. As part of that first step, the source of mismatches between modeled and observed fields is discussed in this work in an effort to establish a starting point for improvements in the modeled thermodynamic field. Model improvements can then be made in parallel with computational advances.

2. Data and model

We have chosen the North Atlantic climatological hydrographic database (Hydrobase) as described by Lozier et al. (1995) for comparison with the numerical model output. Hydrobase was compiled using over eighty years of historical station data (1904–90) from the National Oceanic Data Center. Hydrobase differs from the Levitus and Boyer (1994) and Levitus et al. (1994) World Ocean atlases in that properties are averaged and smoothed on isopycnal surfaces rather than on surfaces of constant depth. As described by Lozier et al. (1994), this choice eliminates the introduction of sizable temperature and salinity anomalies into the database. Because properties are principally advected and mixed along isopycnals, our evaluation of the property fields will focus on their pattern and strength on such surfaces.

The ⅙° Atlantic Ocean model is based on the Parallel Ocean Program (POP) developed at Los Alamos National Laboratory (Dukowicz and Smith 1994). Similar to the Modular Ocean Model (MOM: Pacanowski et al. 1991), the POP model is based on the primitive equation formulation of Bryan (1969) and Cox (1984), but differs from it by treating sea level as a prognostic variable; that is, it uses a free-surface rather than a rigid-lid formulation. In addition to providing a more direct means for comparison with satellite altimetric observations, the free surface POP code runs efficiently on massively parallel computers.

The Atlantic model domain covers 35°S–80°N, 100°W–20°E. This extent allows for the inclusion of deep-water formation in the Greenland–Iceland–Norwegian Sea and Labrador Sea, as well as the formation of intermediate Mediterranean water in the Western Mediterranean Sea. The model's horizontal resolution is approximately ⅙°, which translates into 0.1875° in longitude and 0.1843° in latitude. There are 37 levels in the vertical with 19 levels concentrated in the upper 1000 m. The maximum grid size in the vertical is 250 m. The model was forced by the climatological monthly wind stress and heat flux derived from the European Centre for Medium-Range Weather Forecasts analysis during 1983–86 (Barnier 1995). Sea surface salinity was restored to the Levitus et al. climatology. The water exchange processes across the artificially closed open boundaries are parameterized by 5°-wide buffer zones in which the model temperatures and salinities are restored toward the Levitus et al. (1994) climatology.

The model has been integrated for a total of 34 years starting from a null velocity field and the Levitus et al. climatological January temperature and salinity for each level. Model output during the last 5 years (i.e., model years 30–34) was used to compute the mean fields presented in this work. Due to limited data storage, we were only able to save the full three-dimensional model output at 3-day intervals for years. We decided to save the full three-dimensional fields after model year 30 because we wanted to study the circulation pattern at a time sufficiently distant from the initial model state. Initial results on the model flow fields during this 5-yr period have been presented in Chao et al. (1996), Carton and Chao (1999), and Nakamura and Chao (2001).

During the selected 5-yr period, the volume-integrated kinetic energy per unit area (Fig. 1) shows little or no secular temporal trend, suggesting that the model has established a dynamical equilibrium. The annual cycle evident in Fig. 1 can be attributed to the seasonal variations of the prescribed air–sea fluxes of wind stress, heat, and freshwater.
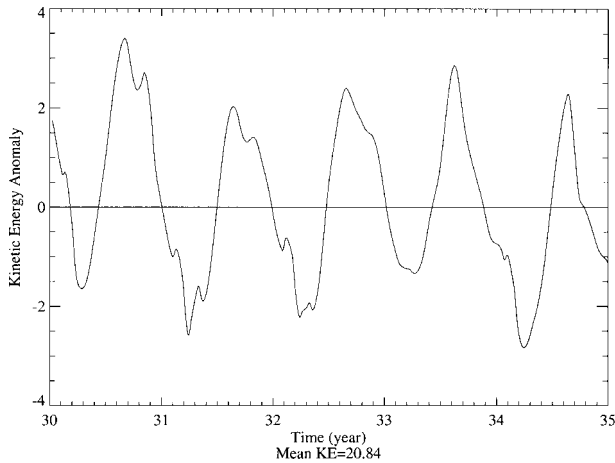
Fig. 1. Time series of volume-averaged kinetic energy per unit area computed over the entire model domain. The 5-yr mean has been removed.

linity fields in the middepth and deep ocean show linear trends in time. The salinity fields at middepth and in the deep ocean are increasing with time. Opposite trends are seen in the temperature fields: the middepth temperature is increasing, while the deep ocean temperature is decreasing with time. The linear trends are 0.007 and −0.001 °C/yr for middepth and deep ocean temperatures, respectively, and 0.001 and 0.0002 psu/yr for middepth and deep ocean salinities, respectively. These slow drifts in the middepth and deep ocean temperature and salinity fields are typical for decade-long integrations of this class of eddy-permitting to eddy-resolving ocean models (Haidvogel and Beckmann 1999). Since the model was initialized with the Levitus et al. climatological January temperature and salinity values, any discrepancy between their January climatology and the model equilibrium state will cause the model's property fields to drift. The discrepancy is likely created by surface forcing and boundary conditions that are not dynamically consistent with the observed thermodynamic state (Haidvogel and Beckmann 1999). While these drifts over 5 years are an order of magnitude smaller than the observed property variability over 80 years (Lozier et al. 1995), their cumulative effect over the years needed to reach equilibrium may be significant. Thus, our analysis of the intermediate and deep property
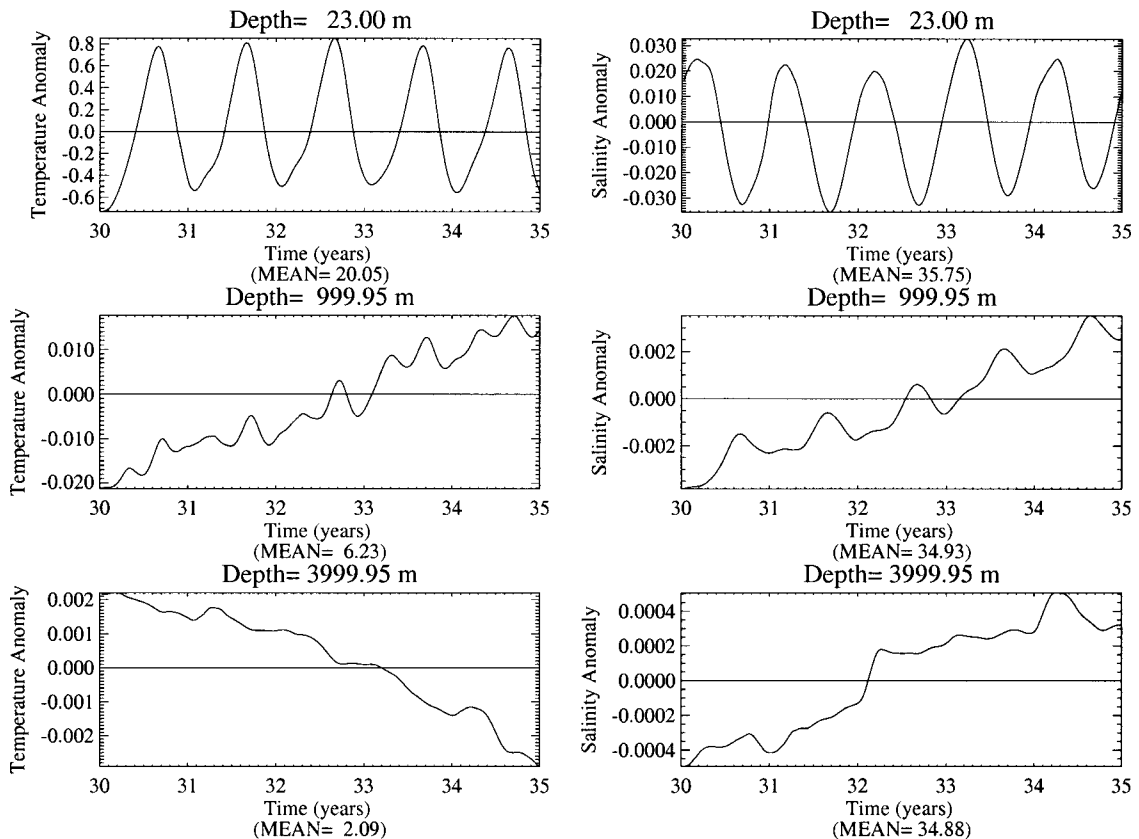
After a 34-yr integration, however, the model has not achieved a thermodynamical equilibrium, as seen by the temporal evolution of the temperature and salinity fields at three selected depths of 23 m, 1000 m, and 4000 m (Fig. 2). While the upper ocean property fields appear to be in a steady pattern, both the temperature and sa-

Fig. 2. Time series of temperature (°C) and salinity (psu) fields averaged over the entire model domain at three selected depths of 23 m, 1000 m, and 4000 m. The 5-yr mean has been removed.

fields will focus only on the gross characteristics of the water masses. It is important to reiterate that we recognize that the equilibrium fields will differ from the fields we show in this paper. However, as will be seen, model/data discrepancies are unlikely to disappear with further model integration.

The mean model-simulated property fields (pressure, temperature, and salinity) were projected onto three constant potential density surfaces ($\sigma_0 = 26.50$, $\sigma_1 = 32.35$, and $\sigma_2 = 36.95$), which are representative of the upper thermocline waters, lower thermocline waters, and deep waters of the subtropical North Atlantic, respectively (Lozier et al. 1995). In order to facilitate the comparison with the observed fields, the model-simulated property maps, at a resolution of $\frac{1}{6}°$, were smoothed to $1°$, the nominal resolution of the observed fields. While the emphasis of this work is principally on the distribution of temperature and salinity on the isopycnals, maps of pressure will be used in this analysis to give an indication of the flow field on an isopycnal. Because the horizontal pressure gradient on an isopycnal is essentially equivalent to the slope of an isopycnal, a pressure map yields the approximate direction of the vertical shear. The horizontal pressure gradient imposed by the sea surface topography is unknown; therefore the pressure gradient deduced from the density field alone (i.e., from the hydrography) yields information on the relative flow field only. If one assumes that the velocity fields goes to zero at a location in the water column (a level-of-no-motion assumption), the isobars approximate absolute flow lines. A deep level-of-no-motion for the subtropical circulation, including the Gulf Stream, its recirculation, and its extension into the North Atlantic Current, is used for the interpretation of the pressure maps in this work. Thus, high pressures are to the right of the flow, looking downstream.

In order to judge the extent to which initialization has affected the model fields, we have included the Levitus salinity field for each of the three selected surfaces. Since the changes in the initial pressure and temperature fields are sufficiently represented by the difference between the Levitus salinity field and the model field (for years 30–34) these fields are not shown. A main reason to show the Levitus fields is to illustrate that the model's ability, or inability, to reproduce the observed property fields is not attributable to the initial conditions.

3. Comparison between the observed and model-simulated property fields on isopycnal surfaces

The observed and modeled pressure, potential temperature, and salinity fields for the $\sigma_0 = 26.50$ surface are displayed in Fig. 3. The model isopycnal is on average about 50–100 m deeper than the 26.50 isopycnal in the North Atlantic; yet this difference is on the order of the observed (Lozier et al. 1995) and modeled (not shown) standard deviation for the pressure field. The subtropical gyre is clearly displayed in both the ob-

served and modeled pressure fields, with the gyre strength somewhat greater in the modeled field. The extent of the subtropical gyre is comparable between the model and data. As seen in the observed field, the gyre is bounded to the west and north by the Florida Current and Gulf Stream, respectively, to the east by a weak southward flow, and to the south by a broad westward return flow. Each of these limbs is reasonably well represented by the model pressure field. The model also reproduces the westward flow of the southern limb into the Caribbean Sea.

Overall, the temperature and salinity fields on this relatively shallow isopycnal are well represented in the modeled fields. Most striking on this density surface is the presence of a large pool of homogeneous water that fills the entirety of the subtropical basin in both the observed and modeled ocean. In the North Atlantic such homogeneity is attributed to the production of the Subtropical Mode Water (McCartney 1982), termed Eighteen-Degree Water (Worthington 1959), near the Gulf Stream front and its subsequent advection into the gyre interior. While the modeled water mass is slightly cooler and fresher, its overall signature represents successful production and distribution of a mode water. As discussed at the end of this section, we believe this favorable comparison is due to the model's ability to simulate the processes that control their formation, not due to the model's initial conditions.

The model also simulates relatively warm and salty water off the northwest coast of Africa, termed Madeira Mode Water in the North Atlantic field. Madeira Mode Water is produced from the local excess of evaporation over precipitation in conjunction with Ekman layer convergence (Siedler et al. 1987). While both Eighteen-Degree water and Madeira Mode Water are identifiable in the modeled fields, there is a much stronger gradient between them than is observed. This difference may result from the difference in temperature and salinity of the two water masses on this surface and/or the differences in the relative strength of advection and diffusion between the ocean and model.

In the subtropical Atlantic Ocean, there is a difference of 0.4 psu between the modeled and observed salinity fields. The initial salinity field from the Levitus et al. climatology (Fig. 4) shows an amplitude comparable to the Hydrobase field (see Fig. 3). Apparently, the model's relaxation to Levitus et al. (1994) sea surface salinity is not strong enough to correct the possible bias in the freshwater flux used in the model.

The intense temperature and salinity gradients that extend eastward from Cape Hatteras delineate a front between the cold, fresh waters to the north and the warm, salty waters to the south in both observed and modeled fields. The front is considerably broader in the observed field, which may result in part from the larger temporal averaging interval for the observed fields. The model and data comparison (see Fig. 3) also reveals other model deficiencies in the upper ocean. For ex-
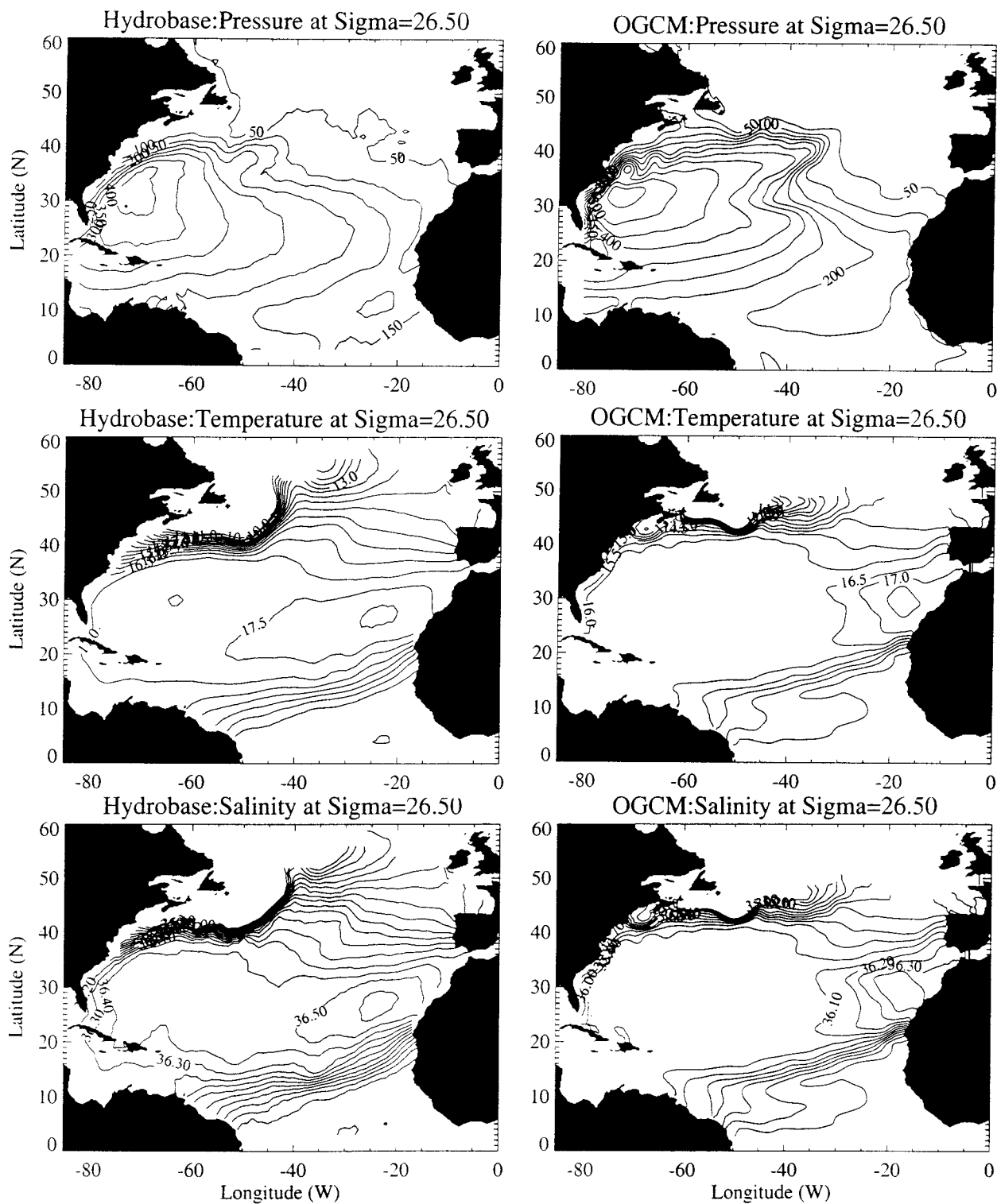
FIG. 3. Mean pressure (m), temperature (°C), and salinity (psu) fields for the $\sigma_0 = 26.50$ surface derived from Hydrobase and model simulation.
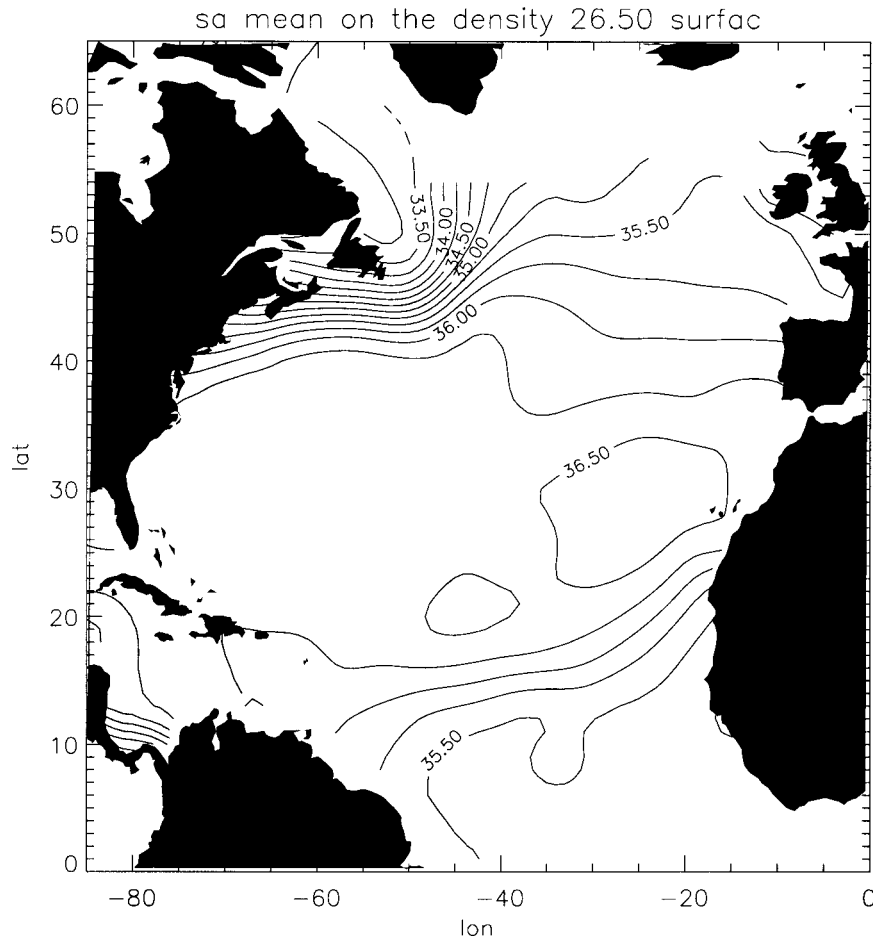
Fig. 4. Mean salinity (psu) field for the $\sigma_0 = 26.50$ surface derived from Levitus et al. (1994) climatology.

ample, an excessively strong, quasi-permanent anticyclonic circulation near the Gulf Stream separation point is evident in the model simulation, an unrealistic feature present in several other eddy-permitting ocean models (Beckmann et al. 1994; Semtner and Chervin 1988; Smith et al. 1992). Farther downstream of the separation point, the isotherms and isohalines from the model Gulf Stream do not turn northward around the Tail of the Grand Banks. These two model deficiencies are mostly due to the lack of eddy forcing at $\frac{1}{6}°$, and are significantly improved in the recent $\frac{1}{10}°$ (Smith et al. 2000) and $\frac{1}{12}°$ (Paiva et al. 1999) calculations. The mesoscale eddy fields, which are dynamically important for the Gulf Stream, are not fully resolved by our $\frac{1}{6}°$ model. Finally, differences are also noted in the outcrop regions for this upper surface, suggesting an investigation into how model outcrops are handled.

Figure 5 shows the observed and modeled pressure, potential temperature, and salinity fields displayed on the $\sigma_1 = 32.35$ surface. The observed pressure field shows a strong Gulf Stream and North Atlantic extension on this surface. The signature of the subtropical

gyre is noticeably absent on this isopycnal because at this depth the flow is weakly depth dependent (Schmitz 1980). In contrast the isobars for the model field do not show a significant signature for the Gulf Stream nor for an extension into the North Atlantic Current. Additionally, the excessively strong meandering near the separation point is still evident at this depth. Unlike the shallower surface, this isopycnal surface, at approximately 1400 m, does not have a sharp thermal or haline front associated with the Gulf Stream and the North Atlantic Current. Instead, the warm and salty Mediterranean Sea Water (MSW) originating from the Strait of Gibraltar completely dominates the property signal in the subtropics. In the observed field the large gradients that are present in the basin interior result from the contrast of this water mass with the much colder and fresher Labrador Sea Water (LSW).

One obvious deficiency in the model simulation is that the origin of the Mediterranean tongue is shifted a few degrees north of the Strait of Gibraltar. The model appears to seriously underestimate the strength of both the LSW and the MSW on this surface. The model's
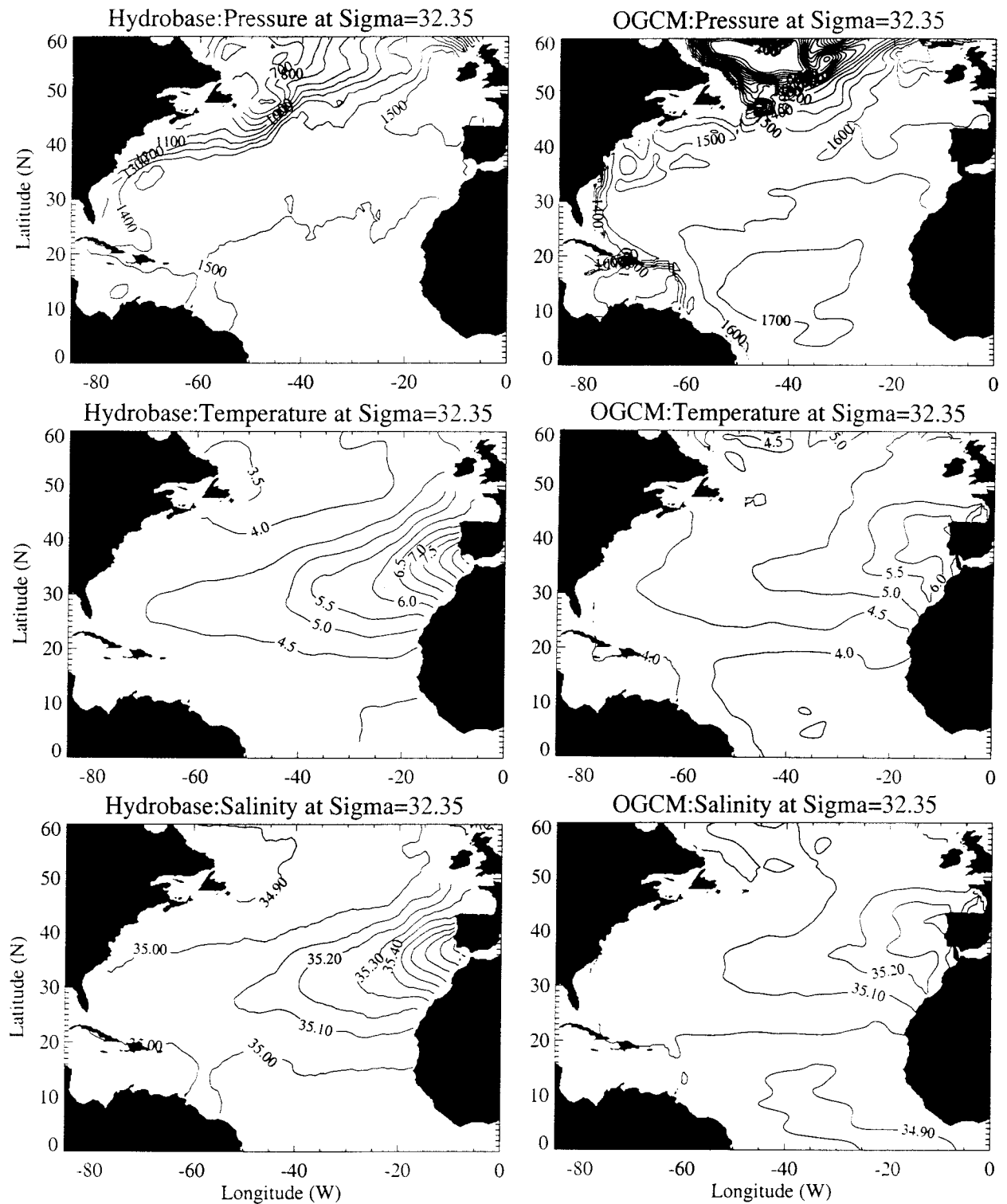
Fig. 5. Mean pressure (m), temperature (°C) and salinity (psu) fields for the $\sigma_1 = 32.35$ surface derived from Hydrobase and the model simulation.

MSW is colder and fresher than observed, while the LSW is considerably warmer and saltier than observed. The combination of colder and fresher MSW and warmer and saltier LSW makes for weak gradients in the model basin interior. However, the cold and fresh water to the south of the Mediterranean tongue (approximately $4.0°$–$4.5°C$ and 35.00 psu), of South Atlantic origin, is well simulated in the model. We attribute this match to the fact that these waters, specified at the southern boundary, spread into the North Atlantic virtually unimpeded by topography. Apparently, overflows (e.g., associated with MSW and LSW) are more problematic, as will be discussed.

The comparison on the deeper surface of $\sigma_2 = 36.95$, as shown in Fig. 6, reveals more discrepancies between the model and data. Noticeably absent in the pressure field is a signature for the deep Gulf Stream and its associated recirculation that are seen in the hydrographic data (Lozier 1997). Unlike the observed fields, the model flow field shows a significant southeastward flow of water extending from the high latitudes into the subtropical basin. Thus, the southwestward flow centered at $30°N$ is associated with this flow of northern waters and not the recirculating deep Gulf Stream waters, as observed in Fig. 6.

The temperature fields on this deep isopycnal differ sharply. Although the model does show a tongue of warm and salty water emanating from the Mediterranean outflow region, as with the previously discussed surface, its origin is more northward than observed. Additionally, the axis of the model advective and diffusive tongue is shifted to the south from the observed axis. The MSW is again cooler and fresher than observed and the high-latitude waters are warmer and fresher. As a result, the gradient field on this surface is also significantly different in the observed and modeled field. For instance, in the western basin the modeled isotherms are nearly orthogonal to the observed ones. The difference in these deep temperature fields suggests that North Atlantic Deep Water (NADW), along with MSW and LSW, are not properly simulated in the model.

An examination of the initial salinity fields on the $\sigma_1 = 32.35$ and $\sigma_2 = 36.95$ surfaces from the Levitus et al. climatology (Fig. 7) shows that the initial amplitude of the Mediterranean tongue is comparable to that given by Hydrobase (Figs. 5 and 6). Thus, the underestimated Mediterranean tongue in the model can be attributed to the model dynamics and/or boundary specifications, and not initial conditions. It is interesting to note that the origin of the Mediterranean tongue on the $\sigma_1 = 32.35$ surface represented by the Levitus et al. climatology (see Fig. 7) is shifted a few degrees north of the Strait of Gibraltar, a feature different from Hydrobase (see Fig. 5). The origin of the Mediterranean tongue on the $\sigma_2 = 36.95$ surface, however, is centered near the Strait of Gibraltar in both the Levitus et al. climatology (see Fig. 7) and Hydrobase (see Fig. 6). Thus, the realignment of the Mediterranean tongue in the modeled salinity field

on both $\sigma_1 = 32.35$ and $\sigma_2 = 36.95$ surfaces are attributed to a combination of initial conditions and model dynamics and/or boundary specifications. An examination of the model velocity field at this depth (not shown) shows a strong northward boundary current, which carries the warm and salty Mediterranean Water far to the north along the Iberian coast before spreading southeastward into the interior.

From an inspection of the Levitus et al. (1994) climatology (Figs. 4 and 7) it is apparent, particularly at depth, that the model has lost most of its "memory" from the initial fields after three decades of model integration. Since the temporal decorrelation scales are expected to increase with depth, a mismatch between the Levitus fields and the model fields at depth indicates that the surface fields are even further from their initialization. Thus, we believe that model dynamics and/or boundary conditions are to be either credited or blamed for the representation of water masses, and not initial conditions.

4. Meridional section of salinity

The water mass structure of the North Atlantic can also be viewed with a meridional section of salinity (Tsuchiya et al. 1992, 1994; Talley 1996). Figure 8 shows a latitude–depth section of annual-mean salinity averaged between $30°$ and $20°W$, for both observed (a) and modeled (b) oceans. Our comparison for this section uses the Levitus et al. climatology since we wish to make the comparison over the whole model domain, which reaches to $35°S$. The effect of the "closed" southern boundary at $35°S$ is clearly evident. Within the buffer zone between $30°$ and $35°S$, the modeled salinity is almost identical to the observed value, because of the strong restoration to the Levitus et al. climatology at all levels. The difference between the observed and modeled salinity fields contributes to the sharp gradient between the model interior and the buffer zone at about $30°S$. This boundary problem becomes less apparent below 500 m.

The major water masses, which contribute to the North Atlantic Ocean circulation, are evident in the observed field as shown in Fig. 8a. The northward inflow through the model's southern boundary at $35°S$ is evident from two low-salinity features: the Antarctic Intermediate Water (AAIW) centered on 900 m and the Antarctic Bottom Water (AABW) below 4000 m. The northward tongue of AAIW penetrates to approximately $20°N$, while AABW penetrates farther northward, to the edge of the section at about $40°N$. Sandwiched between these two water masses of southern origin is the relatively salty NADW, which lies between 1500 and 4000 m. The saline MSW signature lies between $30°$ and $40°N$ centered at about 1000 m. Finally, around $45°$–$60°N$ and between 1500 and 3000 m, a pool of low-salinity LSW is found.
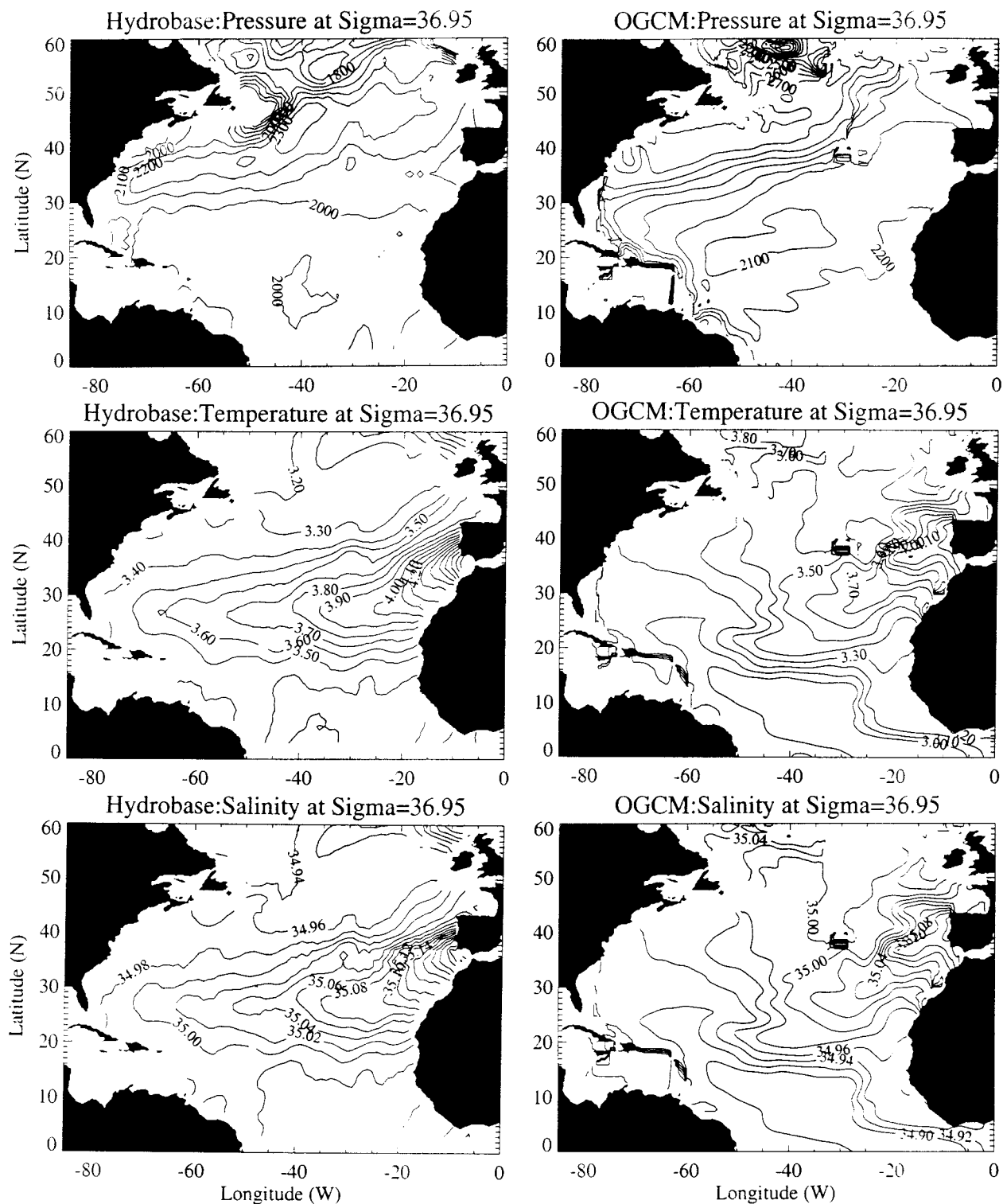
A comparison of the model section (Fig. 8b) with the

Figure 6 shows six contour map panels arranged in a 3×2 grid with titles:

- Hydrobase:Pressure at Sigma=36.95
- OGCM:Pressure at Sigma=36.95
- Hydrobase:Temperature at Sigma=36.95
- OGCM:Temperature at Sigma=36.95
- Hydrobase:Salinity at Sigma=36.95
- OGCM:Salinity at Sigma=36.95

FIG. 6. Mean pressure (m), temperature (°C), and salinity (psu) fields for the $\sigma_2 = 36.95$ surface derived from Hydrobase and the model simulation.
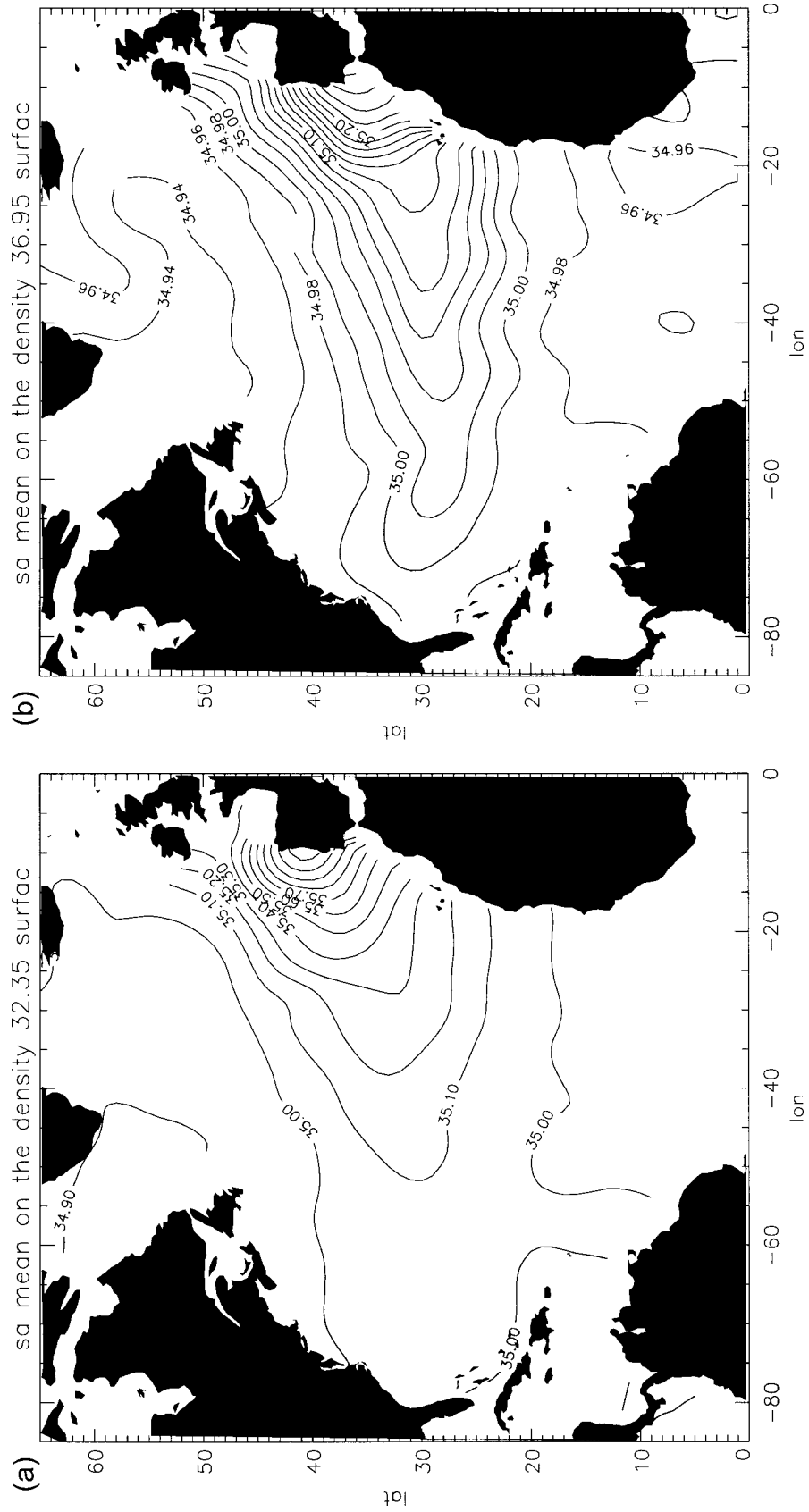
FIG. 7. Mean salinity (psu) fields for the $\sigma_1 = 32.35$ (a) and $\sigma_2 = 36.95$ (b) surfaces derived from the Levitus et al. climatology.
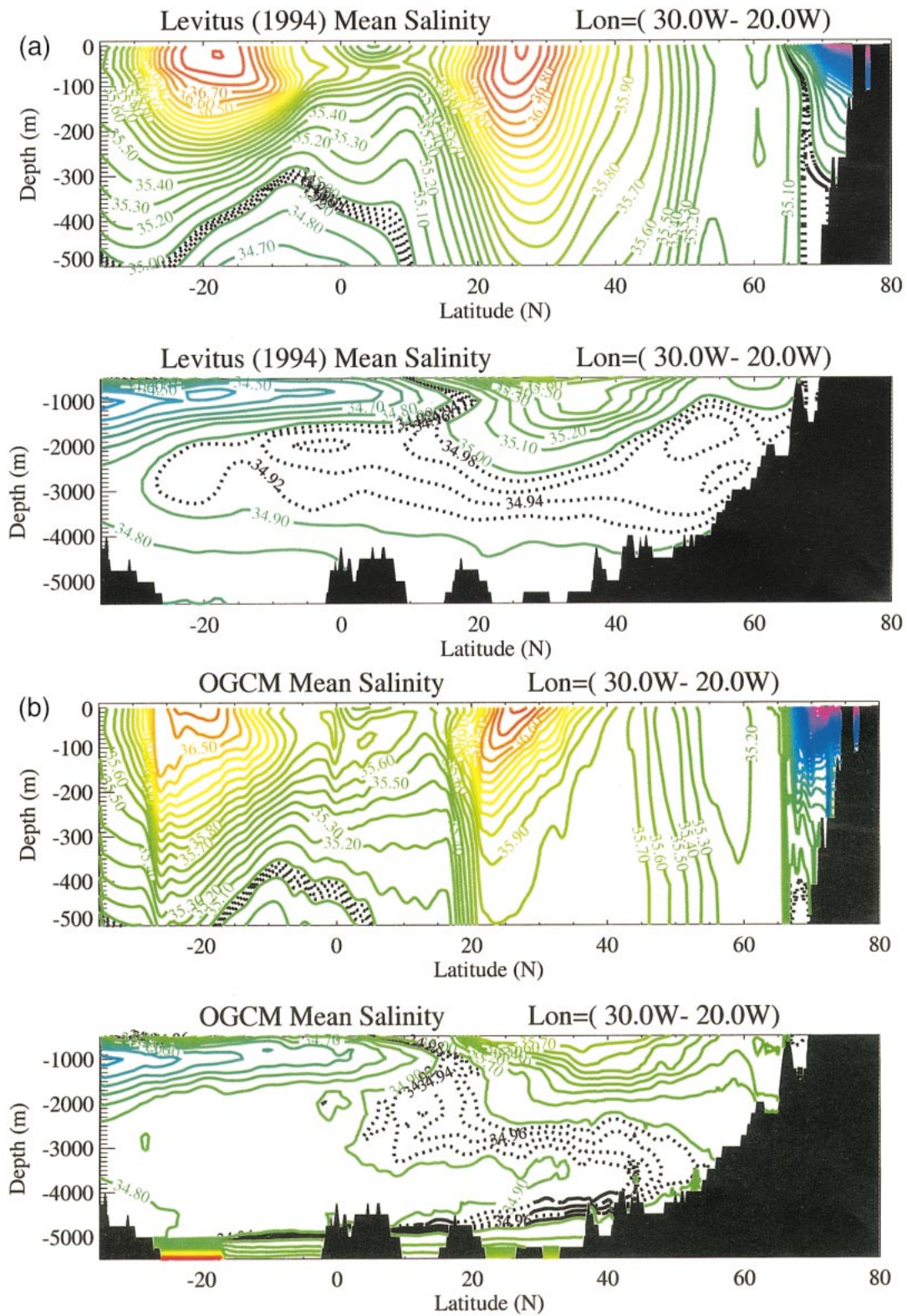
FIG. 8. Latitude–depth section of annual-mean salinity (psu) averaged between 30° and 20°W for the Levitus et al. climatology (a) and the model simulation (b). The upper panels show the depth range from the surface to 500 m, while the lower panels show the depth range from 500 to 5500 m. Red and blue color contours represent high and low salinity values, respectively.
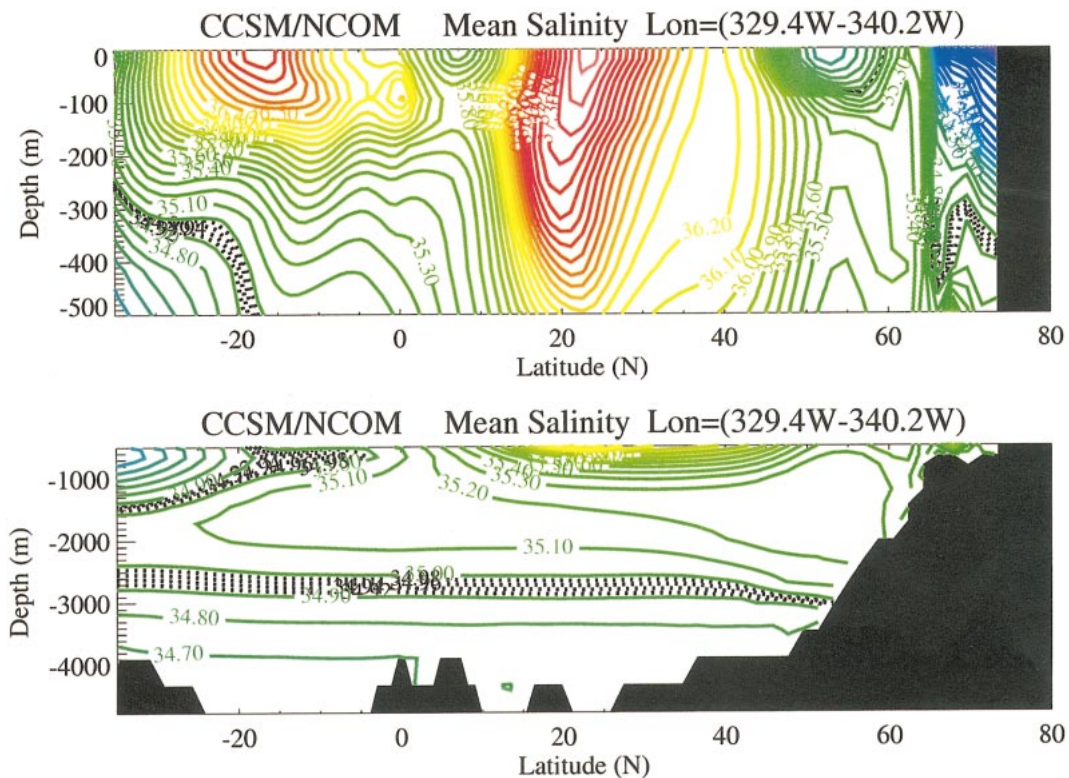
FIG. 9. Latitude–depth section of annual-mean salinity (psu) averaged between 30° and 20°W for the NCOM model simulation. (top) The depth range from the surface to 500 m; (bottom) the depth range from 500 to 5500 m. Red and blue color contours represent high and low salinity values, respectively.

observed section (Fig. 8a) shows that the near-surface salinity is relatively well simulated, with high salinity waters in the subtropical North and South Atlantic and low salinity waters in the northern North Atlantic. This is not surprising since the model surface salinity is restored toward the climatological values (Levitus et al. 1994). However, the modeled salinities in the subtropical North and South Atlantic are still fresher (by 0.3 psu) than the observed, and the modeled salinity in the northern North Atlantic is saltier (by 0.2 psu) than the observed. Also, because of the restoring boundary condition near the southern boundary, the model realistically simulates the AAIW. This modeled water mass lies between 500 and 1500 m, and extends from the southern model boundary to about 15°N.

The modeled MSW, on the other hand, is significantly shallower and occupies a much broader region in the model than is observed. Additionally, the pool of LSW in the northern domain is virtually absent in the model. The NADW penetrates southward only to the equator in the modeled ocean. The modeled AABW, seen as a northward tongue of relatively fresh deep water, is centered at about 4000 m, significantly shallower than the observed AABW. In fact, over much of the North Atlantic basin, the AABW overrides a portion of the NADW such that the bottom water is composed of NADW, rather than AABW, as observed.

Overall, the water masses that fill the North Atlantic basin are identifiable in the model; however, their strength, horizontal penetration, and vertical extent differ substantially from the observed fields. The source of these differences will be discussed in the next section.

It is interesting to see how well a coarse-resolution model that has reached thermodynamic equilibrium represents the deep North Atlantic property fields. Figure 9 shows the meridional section of salinity as derived from the National Center for Atmospheric Research (NCAR) Community Climate System Model (CCSM) Ocean Model (NCOM) [see Gent et al. (1998) for a description of model details and experiment design]. As seen in Fig. 9, the NCOM fields fare far worse than our model fields in the representation of the deep property fields. In our model fields, AABW and NADW are distinct, whereas such a distinction cannot be made in the NCOM fields. These deep water masses are located at approximately the correct depths in our model fields, whereas in the NCOM fields NADW is apparently spreading with its core centered at 1800 m, far above the observed core in the Levitus section. Additionally, below approximately 2000 m in the NCOM section the isohalines are essentially flat, showing little, if any, latitudinal gradient. However, since we do not know the extent to which our model fields at a full thermodynamic equilibrium would differ from these fields at year 34,

we cannot necessarily attribute improvement over the NCOM fields to improved model formulation (e.g., higher resolution). In fact, it may be that the eddy-resolving model has simply not had the time to drift as far as the NCOM model. Our main objective in this comparison (between the NCOM fields and ours) is to illustrate that, while thermodynamic equilibrium is desirable, the current ability to attain thermodynamic solutions that have realistic property fields is lacking. As stated earlier, an investigation of the evolution of property fields from the NCOM model reveals that deficiencies in the property fields can be detected before a full thermodynamic equilibrium is achieved. Thus, we believe there is merit to evaluating the property fields simulated by an eddy-permitting model before reaching full thermodynamic equilibrium.

5. Discussion and summary

Overall, the upper ocean property fields are relatively well simulated, yet the middepth and deep ocean property fields are poorly represented in the ⅙° Atlantic Ocean model that has been integrated to 34 years. A representative simulation of an observed property field hinges on many aspects of the model, including adequate boundary conditions and the correct balance between advection and diffusion and between mean and eddy components. Our evaluation of the modeled property fields points out two possible problems in the model: 1) improper boundary specifications of water masses and 2) inadequate treatments of bottom boundary layer processes. Each of these will be discussed in turn.

The "closed" model boundary is approximated by the buffer zone (or sponge layer) where the model temperature and salinity are restored toward the Levitus et al. climatology. It is known that the Levitus et al. climatology was obtained by applying heavy averaging along isobaric surfaces. Such averaging, by essentially mixing surrounding waters with the "boundary waters," could produce the observed dilution of the model's NADW, LSW, and MSW. It would be desirable to specify the boundary conditions using Hydrobase (Lozier et al. 1995). Hydrobase is gridded on isopycnal surfaces with smaller averaging scales and has the advantage that it preserves the original temperature–salinity characteristics of the raw hydrographic data. Thus, before one can assess whether the model does an adequate job distributing the water mass from its origin, it is essential to adequately represent the water masses at their point of entry into the model domain. Hydrobase has not been used for our model boundary conditions simply because of its limited spatial coverage over the North Atlantic Ocean from equator to 60°N. It is expected that a global Hydrobase 2, to be released in early 2001 (R. Curry 2001, personal communication), will be very useful for model boundary specification and for model/data comparison.

Another major problem in the model is the poor model representation of bottom boundary layer processes (e.g., flow over topography). The staircase representation of the bottom topography used in z-coordinate ocean models (e.g., MOM and POP) tends to diffuse property fields, thus preventing the deep water from reaching the deep ocean. For example, the poor representation of the overflow processes through the Denmark Strait west of Iceland, the Iceland–Faroe Ridge east of Iceland, and the Faroe–Shetland Channel farther to the east contribute to mismatches between the modeled and observed fields. During the past few years, there have been several bottom boundary layer schemes (Beckmann and Döscher 1997; Killworth and Edwards 1999; Döscher and Beckmann 2000; Song and Chao 2000; Doney and Hecht 2001, manuscript submitted to *J. Phys. Oceanogr.*) designed to improve the topographic representation in z-coordinate ocean models. It is expected that the implementation of a bottom boundary layer scheme in the ⅙° Atlantic model should significantly improve the property field simulations in both the overflow region and the model interior.

In addition to evaluating property field simulations with our improved specifications of water masses and bottom boundary layer parameterizations, it is important to perform the type of data and model comparisons presented in this paper with other eddy-permitting to eddy-resolving simulations (e.g., Smith et al. 2000). Given the limited computing resources available for these high-resolution simulations (Semtner 1995), it would be cost effective to implement the measures necessary to improve property field representations as early as possible during the model integration and/or before increasing the horizontal resolution even further. Ultimately, improved property field simulations will lead to improved simulations of the flow field, particularly in the deep ocean.

REFERENCES

Barnier, B., L. Siefridt, and P. Marchesiello, 1995: Thermal forcing for a global ocean circulation model from a three-year climatology of ECMWF analysis. *J. Mar. Syst.,* **6,** 363–380.
Beckmann, A. C., and R. Döscher, 1997: A method for improved representation of dense water spreading over topography in geopotential-coordinate models. *J. Phys. Oceanogr.,* **27,** 581–591.
——, ——, C. Koberle, and J. Willebrand, 1994: Effects of increased horizontal resolution in a simulation of the North Atlantic Ocean. *J. Phys. Oceanogr.,* **24,** 326–344.

Bryan, F. O., and W. R. Holland, 1989: A high resolution simulation of the wind and thermohaline-driven circulation in the North Atlantic Ocean. *Parameterization of Small-Scale Processes: Proc. 'Aha Huliko'a Hawaiian Winter Workshop,* Manoa, HI, University of Hawaii, 99–115.

Bryan, K., 1969: A numerical method for the study of the world ocean circulation. *J. Comput. Phys.,* **4,** 1687–1712.

Carton, J. A., and Y. Chao, 1999: Caribbean Sea eddies inferred from TOPEX/POSEIDON altimetry and a ⅙° Atlantic Ocean model simulation. *J. Geophys. Res.,* **104,** 7743–7752.

Chao, Y., A. Gangopadhyay, F. O. Bryan, and W. R. Holland, 1996: Modeling the Gulf Stream system: How far from reality? *Geophys. Res. Lett.,* **23,** 3155–3158.

Cox, M. D. 1984: A primitive equation, 3-dimensional model of the ocean. Ocean Group Tech. Rep. 1, Geophysical Fluid Dynamics Laboratory, Princeton, NJ, 143 pp.

Döscher, R., and A. Beckmann, 2000: Effects of a bottom boundary layer parameterization in a coarse resolution model of the North Atlantic Ocean. *J. Atmos. Oceanic Technol.,* **17,** 698–707.

Dukowicz, J. K., and R. D. Smith, 1994: Implicit free-surface method for the Bryan–Cox–Semtner ocean model. *J. Geophys. Res.,* **99,** 7991–8014.

DYNAMO Group, 1997: DYNAMO: Dynamics of the North Atlantic Models: Simulation and assimilation with high-resolution models. Institut für Meereskunde Rep. 294, Universitat Kiel, Kiel, Germany, 334 pp.

Gent, P. R., F. O. Bryan, G. Danabasoglu, S. C. Doney, W. R. Holland, W. G. Large, and J. C. McWilliams, 1998: The NCAR Climate System Model Global Ocean Component. *J. Climate,* **11,** 1287–1306.

Haidvogel, D. B., and A. Beckmann, 1999: *Numerical Ocean Circulation Modeling.* Imperial College Press, 330 pp.

Killworth, P. D., and N. R. Edwards, 1999: A turbulent bottom boundary layer code for use in numerical ocean models. *J. Phys. Oceanogr.,* **29,** 1221–1238.

Levitus, S., and T. P. Boyer, 1994: *World Ocean Atlas 1994.* Vol. 4: *Temperature, NOAA* Atlas NESDIS, 117 pp.

——, R. Burgett, and T. P. Boyer, *World Ocean Atlas 1994.* Vol. 3: *Salinity, NOAA* Atlas NESDIS, 99 pp.

Lozier, M. S., 1997: Evidence for large-scale eddy-driven gyres in the North Atlantic. *Science,* **277,** 361–364.

——, M. S. McCartney, and W. B. Owens, 1994: Anomalous anomalies in averaged hydrographic data. *J. Phys. Oceanogr.,* **24,** 2624–2638.

——, W. B. Owens, and R. G. Curry, 1995: The climatology of the

North Atlantic. *Progress in Oceanography,* Vol. 36, Pergamon, 1–44.

McCartney, M. S., 1982: The subtropical recirculation of mode water. *J. Mar. Res.,* **40** (Suppl.), 427–464.

McWilliams, J. C., 1995: Modeling the ocean general circulation. *Annu. Rev. Fluid Mech.,* **28,** 215–248.

Nakamura, M., and Y. Chao, 2001: Diagnoses of an eddy-resolving Atlantic Ocean model simulation in the vicinity of the Gulf Stream. Part I: Potential vorticity. *J. Phys. Oceanogr.,* **31,** 353–378.

Pacanowski, R., K. Dixon, and A. Rosati, 1991: Modular Ocean Model users' guide. Ocean Group Tech. Rep. 2, Geophysical Fluid Dynamics Laboratory, Princeton, NJ, 16 pp.

Paiva, A. M., J. T. Hargrove, E. P. Chassignet, and R. Bleck, 1999: Turbulent behavior of a fine mesh ($1/12$°) numerical simulation of North Atlantic. *J. Mar. Syst.,* **21,** 307–320.

Schmitz, W. J., 1980: Weakly depth dependent segments of the North Atlantic circulation. *J. Mar. Res.,* **38,** 111–133.

Semtner, A. J., 1995: Modeling ocean circulation. *Science,* **269,** 1379–1385.

——, and R. M. Chervin, 1988: A simulation of the global ocean circulation with resolved eddies. *J. Geophys. Res.,* **93,** 15 502–15 522.

Siedler, G., A. Kuhl, and W. Zenk, 1987: The Madeira Mode Water. *J. Phys. Oceanogr.,* **17,** 1561–1570.

Smith, R. D., J. K. Dukowicz, and R. C. Malone, 1992: Parallel ocean circulation modeling. *Physica D,* **60,** 38–61.

——, M. E. Maltrud, F. O. Bryan, and M. W. Hecht, 2000: Numerical simulation of the North Atlantic Ocean at $1/10$°. *J. Phys. Oceanogr.,* **30,** 1532–1561.

Song, Y. T., and Y. Chao, 2000: An embedded bottom boundary layer formulation for z-coordinate ocean models. *J. Atmos. Oceanic Technol.,* **17,** 546–560.

Talley, L. D., 1996: North Atlantic circulation and variability, reviewed for the CNLS conference. *Physica D,* **98,** 625–646.

Tsuchiya, M., L. D. Talley, and M. S. McCartney, 1992: An eastern Atlantic section from Iceland southward across the equator. *Deep-Sea Res.,* **39,** 1885–1917.

——, ——, and ——, 1994: Water mass distributions in the western South Atlantic: A section from South Georgia Island (54S) northward across the equator. *J. Mar. Res.,* **52,** 55–81.

Willebrand, J., and Coauthors, 2001: Circulation characteristics in three eddy-permitting models of the North Atlantic. *Progress in Oceanography,* Vol. **48,** Pergamon, 123–161.

Worthington, L. V., 1959: The 18° water in the Sargasso Sea. *Deep-Sea Res.,* **5,** 297–305.